Rheological Studies and Numerical Investigation of Barite Sag Potential of Drilling Fluids with Thermochemical Additive Using Computational Fluid Dynamics (CFD)

Dr. Olalekan Alade, Dr. Mohamed Mahmoud and Ayman R. Al-Nakhli

Abstract /

A novel method of improving the rheological performance of drilling fluids, water-based mud (WBM) against barite particle settling, otherwise known as barite sag, has been developed. This method involves adding a certain quantity of thermochemical fluid to the fluid to increase the temperature and increase viscosity. We have substantiated this claim experimentally by conducting rheological tests and theoretically using computational fluid dynamics (CFD) simulation. WBM, with encapsulated thermochemical fluid (TCF), was prepared. Rheological tests were conducted under low and high temperature ranges.

The experimental data from rheological studies have been employed to guide CFD modeling and simulation of multiphase flow of a dense suspension, mimicking the conventional WBM, and those comprising thermochemical fluids (additives) (WBM_TCF). The results revealed that the drilling fluids conformed to the shear thinning pseudoplastic behavior within the operational conditions described in this study. Notably, the apparent viscosity of the WBM was observed to decrease with increasing temperature between 25 °C and 50 °C, but increased afterward. At higher temperatures, 20 °C to 70 °C, which corresponds to the conditions of the newly formulated muds, it was found that the WBM_TCF exhibits a lower potential for barite sag due to lower settling velocity of the particles. The reason essentially has to do with a higher viscosity of the WBM_TCF.

The CFD studies have considered both the hydrodynamic forces and shear induced migration of the particles. Analyses of various simulation results, including particle flux, particle mass fraction, mixture viscosity, and the pressure drop, consistently revealed that the WBM_TCF might have lower barite segregation potentials compared with other types of drilling fluids considered in this study.

Introduction

Particulate segregation is a popular phenomenon in the drilling operations. At different flow regimens, the solid components of the drilling fluids tend to segregate under the influence of various factors, including the physical properties of the particles viz. size, shape, and density, properties of the dispersing fluid and operating conditions[1]. The settling and/or sagging of weighting materials in drilling fluids is a major concern when drilling and completing a well[2]. The segregation of the barite weighting component of the drilling fluid, commonly referred to as barite sag, can lead to various complications such as annular pressure buildup and control problems, stuck pipes, plugged boreholes and lost circulation, problematic cement jobs, etc.[3, 4]. Separation of weighting materials in a non-moving fluid column is referred to as static sag while sag in a flowing fluid is normally referred to as dynamic sag[2]. All along, the operational consequences of barite sag can be equally severe under both static and dynamic conditions[1].

Mud properties, including rheology, density, properties of the weighting material, and chemical treatments were the key factors affecting barite sag phenomenon[5]. Incidents with sag of solid weighting agents in drilling fluids can lead to potential drilling impediments, including loss of wellbore control, lost circulation, stuck pipe, and high torque. The presence of sag has relatively often been the cause for gas kicks, and oil-based muds (OBM) are known to be more vulnerable for sag than WBMs[2]. Barite sag is caused by the settling of suspended barite particles, which can lead to a variation in drilling fluid density[6]. The study of barite sag mechanisms essentially plays a key role in developing field guidelines to manage the consequences[7].

Furthermore, an adequate knowledge of drilling fluid behavior ultimately enables successful operations[8]. Therefore, several investigations have been dedicated toward solving barite sag problems[9]. In addition, various techniques have been developed for detecting particle sagging potential in drilling fluids, which range from the standard viscometer to lab-scale flow loops[10]. Accordingly, many of these studies employed experimental approaches to evaluating barite sag problems as related to the rheology of the drilling fluids[9].

Ofei et al. (2020)[2] examined the effects of rheological and viscoelastic properties of typical field OBMs on barite sag performance under static and dynamic conditions. Essentially, their investigation presented an approach to

obtain static and dynamic barite sag measurement protocols using the rheological and viscoelastic properties of typical field OBM. Static sag results are computed based on a modified Stokes settling theory while dynamic sag results are compared for rotational and oscillatory ultra-low to low shear conditions.

Further, various investigations were conducted[5,11] that generally considered the influence of fluid rheology and flow temperature on the barite sag. Other reports on the laboratory-scale investigation of barite sag phenomenon[12-14], studied barite sag under dynamic conditions using rheological analysis incorporating flow loop experiments. Bern et al. (2000)[7] studied barite sag mechanisms and developed field guidelines to manage the consequences. The results revealed that the influencing factors such as physical properties of the mud, wellbore conditions, and characteristics of the weighting materials are interrelated and seldom act in isolation.

The growing advancements in drilling technology and diverse operational requirements have brought significant complexity to the formulation of the drilling fluids[15]. One such innovative idea to improve operational performance of drilling fluids includes encapsulation of thermochemical fluid (TCF) in the mud formulation with the purpose of generating heat during the operation. Essentially, the heat generated is expected to enhance the dissolution and/or removal of the filter cake, which can be formed during drilling operations[16].

In the study[16], we proposed a formulation in which the TCF was used as an additive in both OBM and WBM. Therefore, the focus of the present study is to investigate barite sagging of the drilling fluid with encapsulated TCF (WBM_TCF). For this purpose, the computational fluid dynamic (CFD) technique has been applied with the rheological characteristics of the base fluids (WBM). As a contribution to knowledge in this regard, we are also incorporating thermal activation energy, due to the effect of temperature on the fluid rheology, in the CFD simulation scheme.

Rheological Modeling of the Drilling Fluids with TCF Additives

The detailed formulation of WBM drilling fluids used in this study has been presented elsewhere[16]. The old conventional drilling fluids (WBM) were prepared without TCF, while the newly developed formulation is encapsulated with the TCF. This new formulation herein is named WBM_TCF with regard to the WBM base formulation, respectively. As previously stated, the new formulation of the drilling fluid is expected to form a self-destructive mud cake by releasing heat due to the exothermic reaction of the TCF additives.

Figure 1 shows the TCF reaction, which is expected to cause a temperature rise, and simultaneously increase in the pressure of the system, typically up to 120 °C and 250 psi, when triggered at 70 °C.

The viscosity of the drilling fluids was measured using the Anton Paar Rheometer/Dynamic Mechanical Analyzer (MCR 702) at different temperatures and shear rates (0.001 to 1,000 s^{-1}). The flow behavior of the fluids was evaluated by fitting the data to the two-parameter power law, Ostwald-de-Wale model[17,18] function. Therefore, the flow consistency index, K, and the flow behavior index, n, were calculated from the apparent viscosity, μ_a, and shear rates, $\dot{\gamma}$, using Eqns. 1 and 2, as follows:

$$\mu_a = K\dot{\gamma}^{n-1} \quad (1)$$

$$\ln\mu_a = \ln K + (n-1)\ln\dot{\gamma} \quad (2)$$

The temperature dependency of the viscosity (otherwise known as thermal effect) was evaluated from the Arrhenius equation, Eqn. 3:

$$K = K_0 exp\left(\frac{E_a}{RT}\right) \quad (3)$$

where K_o is the system dependent pre-exponential factor, and E_a is the flow activation energy, defined through Eqn. 4.

$$R\frac{dln\mu_a}{dT^{-1}} \quad (4)$$

Therefore, E_a was obtained by plotting lnK vs. T^{-1} and multiplying the slope by the universal gas constant R (8.3144598 $Jmol^{-1}K^{-1}$).

Subsequently, a new expression to calculate the viscosity of the drilling fluid, based on the thermal effect, was developed, Eqn. 5:

$$\mu_a = K_0 exp\left(\frac{E_a}{RT}\right)\dot{\gamma}^{n-1} \quad (5)$$

Gravitational Settling of Particles (Hindered Settling Velocity: V_{STH})

For a rigid particle moving through a fluid, there are three acting forces: (1) the gravitational force, (2) the buoyant force, which acts parallel with the external force but in the opposite direction, and (3) the drag force, which appears whenever there is relative motion between the particle and the fluid.

For a single particle of mass, m, moving in a fluid, the

Fig. 1 *The temperature and pressure released from a typical thermochemical reaction triggered at 70 °C.*

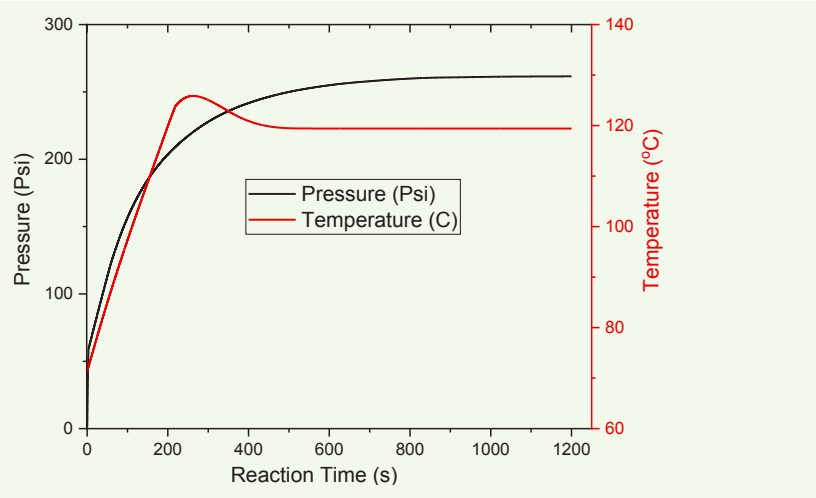

net force, F, acting on the particle, can be defined as the total of the downward force of gravity, F_e, the force of drag, F_d, and the buoyancy, F_b. Then, when the terminal velocity is reached, the settling velocity of the particle becomes asymptotic to a constant value with the net acceleration = 0. From the above statements, by Eqns. 6a to 6e, it can be deduced that:

$$F = F_e - F_b - F_d \quad (6a)$$

$$F = m\frac{dV}{dt} \quad (6b)$$

$$F_e = ma_e \quad (6c)$$

$$F_b = \frac{m\rho_f a_e}{\rho_p} \quad (6d)$$

$$F_d = \frac{C_D A_p \rho_f V^2}{\rho_p} \quad (6e)$$

When the net acceleration = 0, the terminal velocity, V_t, is obtained from Eqn. 7, as follows:

$$V_t = \left(\frac{2g(\rho_p - \rho_f)}{A_p \rho_P C_D \rho_f}\right)^{1/2} \quad (7)$$

where A_p, ρ_p, ρ_f, and C_D are the surface area of the particle, density of the particle, density of the fluid, and the drag coefficient, respectively.

Then, for a spherical particle diameter, D_p, the terminal velocity is given by Eqn. 8:

$$V_t = \left(\frac{4gD_p(\rho_p - \rho_f)}{3C_D\rho_f}\right)^{1/2} \quad (8)$$

For the case of creeping flow (flow at very low velocities relative to the sphere), the F_d on the particle can be obtained through the Navier-Stokes equations. Now, for $R_{ep} < 1$, the F_d, the C_D, and therefore, the V_t can be obtained from Eqns. 9, 10, and 11, respectively.

$$F_d = 3\pi\mu V_t D_p \quad (9)$$

$$C_D = \frac{24}{R_{ep}} \quad (10)$$

$$V_t = \frac{gD_p{}^2(\rho_p - \rho_f)}{18\mu_f} \quad (11)$$

For a power law fluid in the Stoke's law range, the particle's Reynolds number, N_{Rep}, is calculated from the average settling velocity, $\overline{V}_{STH}$, using Eqn. 12:

$$R_{ep} = \frac{\rho_f \overline{V}_{STH}^{2-n} D_p^n}{K} \quad (12)$$

where K and n are the flow parameters obtained from the Power Law rheological model.

The hindered settling velocity, V_{STH}, can be calculated from the terminal velocity of a single particle, V_t, using Eqn. 13[19]:

$$V_{STH} = V_t(v)^{\omega} \quad (13)$$

where v and ω are the void fraction and system specific exponent, respectively.

Computational Methodology: CFD Modeling and Simulation of Barite Segregation

Drilling fluids are a colloidal suspension comprised of solid particles suspended in a continuous liquid phase. The flowing suspensions of particles in a liquid have been known to exhibit particle migration even in creeping flow and in the absence of significant nonhydrodynamic or gravitational effects[20]. When subjected to the action of a moving fluid, particles experience various settling characteristics, which is induced by gradients in shear rate, concentration, and relative viscosity. From these perspectives, a constitutive model otherwise referred to as the diffusive flux model, for the evolution of particle concentration in a flowing suspension, was proposed by Phillips et al. (1992)[21].

Accordingly, Rao et al. (2002)[22] applied a continuum constitutive equation based on the diffusive flux using the finite element method (FEM) to examine the performance of suspended particles, both in batch sedimentation and in shear between concentric rotating cylinders. Numerical results were complemented with experimental data of batch sediment and those of 2D nuclear magnetic resonance imaging measuring the evolution of solid fraction profiles in the same suspension undergoing flow between rotating concentric cylinders. The present scenario is a multiphase flow involving liquid and solid. In this case, the presence of different phases is described using the volume fractions, while interphase effects such as surface tension, buoyancy, and transport across phase boundaries are treated using the dispersed multiphase flow models.

Numerical modeling adopted in the COMSOL multiphysics uses a macroscopic two-phase model in which volume fractions of the phases are tracked. The mixture model based on the diffusive flux is set up in the laminar flow interface. The mathematical model[22, 23] comprises a set of partial differential equations, including the momentum transport equation for the mixture, Eqn. 14, a continuity equation, Eqn. 15, and a transport equation for the solid-phase volume fraction, Eqn. 16:

$$\rho\frac{\partial j}{\partial t} + \rho(j.\nabla)j = -\nabla P - \nabla.\left(\rho c_p(1 - c_p)u_{slip}u_{slip}\right) + \nabla.\mu[(\nabla j + \nabla j^T)] + \rho g \quad (14)$$

where j is the volume averaged mixture velocity, P is the pressure, c_s is the dimensionless particle mass fraction, and u_{slip} is the relative velocity between the solid and the liquid phases.

The continuity equation for the mixture model is given as:

$$(\rho_f - \rho_p)\left[\nabla.\left(\emptyset_p(1 - c_s)u_{slip}\right)\right] + \rho_f(\nabla.u) = 0 \quad (15)$$

where ρf and ρp are the densities of the fluid and solid phase (particle), respectively. The solid phase volume fraction is denoted by $\emptyset_p$.

The transport equation for the solid-phase volume fraction is given as:

$$\frac{\partial}{\partial t}\left(\rho_p\emptyset_p\right) + \nabla.\left(\rho_p\emptyset_p u_p\right) = 0 \quad (16)$$

The solid-phase velocity, u_p, the relative velocity, u_{slip}, and the particle flux, j_p, were defined, Eqns. 17 to 19, as:

$$u_p = u + (1 - c_S)u_{slip} \quad (17)$$

$$u_{slip} = \frac{j_p}{\emptyset_p \rho_p (1-c_s)} \quad (18)$$

$$\frac{j_p}{\rho_p} = -[\emptyset D_\emptyset \nabla(\dot{\gamma}\emptyset) + \emptyset^2 \dot{\gamma} D_n \nabla(ln\mu)] + f_h V_t \emptyset \quad (19)$$

where $D_\emptyset$ and D_n are empirically fitted parameters. V_t and V_h are the settling velocity and hindering functions, respectively.

The density, ρ_m, of the mixture[22] was calculated using simple mixing rule, Eqn. 20:

$$\rho_m = (1 - \emptyset_p)\rho_f + \emptyset_p \rho_p \quad (20)$$

The viscosity, μ_m, was calculated using the Krieger-Dougherty derived empirical correlation, Eqn. 21, presented as[24]:

$$\mu_m = \mu_f \left(1 - \frac{\emptyset_p}{\emptyset_m}\right)^{-2.5\emptyset_m} \quad (21)$$

where μ_f is the fluid's viscosity, and $\emptyset_m$ is the maximum packing concentration.

The solution of these equations describes the dynamics of the system. The detailed of typical solution algorithm had been presented elsewhere in the literature[22, 23]. The multiphysics involves coupled laminar flow and phase transport interfaces. The equations were discretized by using the FEM in the multiphase mixture model of COMSOL software. Figures 2 and 3 are the computational geometry used in the CFD analysis. The simulation parameters are listed in Table 1.

Results and Discussion

Rheological Characteristics of Drilling Fluids

The apparent viscosity and temperature relationship of the WBM is presented in Fig. 4, respectively. From Fig. 5, it can be observed that the apparent viscosity of the WBM deceases with an increasing temperature between 25 °C to 50 °C. Subsequently, the apparent viscosity tends to increase after 50 °C up to 90 °C, at all shear rates. The reason for this behavior might be due to the decrease in stability of the WBM at higher temperatures. Furthermore, it can be observed that the reduction in viscosity due to shear rates is more pronounced at the lower shear rates — 0.06 s^{-1} to 0.7 s^{-1} — compared with the shear rates above 1 s^{-1}, at all temperatures. It is expected that the viscosity of colloidal dispersion, such as drilling fluids, would become less sensitive to the shearing force or temperature due to increased homogeneity[25].

Additionally, Fig. 5 presents the rheological behaviors. It shows that the shear stress increased with the rate of

Fig. 3 *A 2D diagram of the Couette device showing the section through which the parameters were analyzed.*

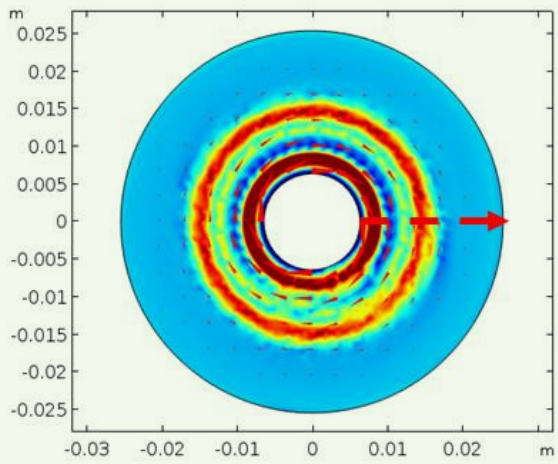

Fig. 2 *A 3D illustration of a Couette device, which consists of two coaxial cylinders (left), and (right), a 2D meshed Couette device with a radii of 0.0064 m and 0.0254 m, for the inner and outer cylinders, respectively.*

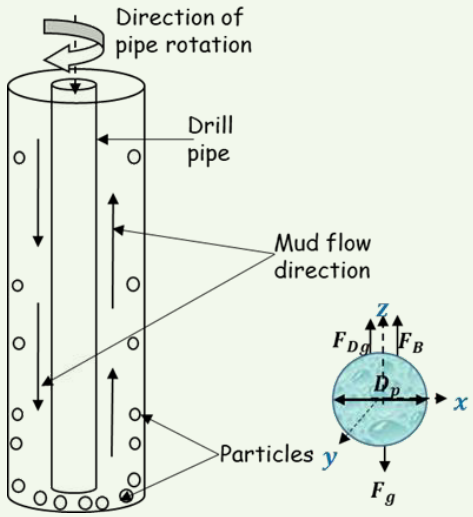

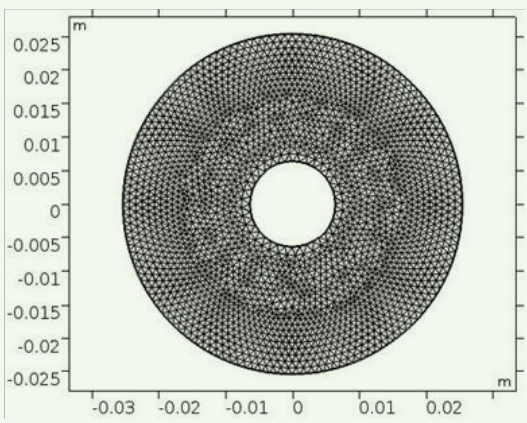

Table 1 *The simulation parameters.*

	OBM	OBM_TCF	WBM	WBM_TCF
Density of particle: barite (kg/m^3)	4,200	4,200	4,200	4,200
Density of fluid (kg/m^3)	828	764	1,100	1,045
Particle radius (m)	2.50E-05	2.50E-05	3.00E-05	3.00E-05
Particle sphericity	1	1	1	1
Initial values				
Velocity (m/s); x, y	0			
Pressure (Pa)	0			
RPM (min^{-1})	3; 6; 10; 100; 300			
Rotation time (min)	60			

Fig. 4 *The apparent viscosity vs. temperature of the WBM at different shear rates.*

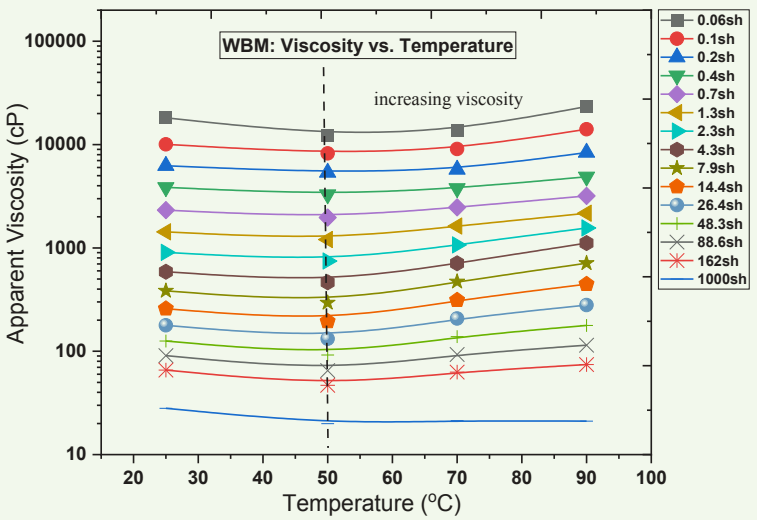

shearing, between 25 °C and 50 °C shearing temperatures, but above that, from 70 °C to 90 °C, the shear stress increased. This observation is consistent with the viscosity temperature behavior, which was explained earlier, Fig. 4. To further support the above observations, the temperature ramp test was performed for the fluids at s constant shear rate of 200 s^{-1}. In accordance with the temperature response earlier discussed, Fig. 6 shows that the apparent viscosity of OBM decreases with increasing temperature. Closely related to the observation earlier presented, the apparent viscosity of the WBM increased significantly after 50 °C.

Thermal Effect: Assessment of Rheological Characteristics of WBM_TCF

As presented in a previous publication[16], the new formulations — WBM_TCF — show very similar rheological characteristics at low temperature, i.e., below the 70 °C activation temperature. After activation, the fluids are expected to exhibit rheological behavior consistent with those of the conventional base drilling fluids, i.e., WBM, at higher temperatures, above 70 °C.

Therefore, the rheological characteristics of the WBM_TCF have been assessed using Eqn. 5, and with the assumption of the temperature change of the TCF reaction previously shown in Fig. 1. Table 2 lists the estimated rheological parameters. The data presented in the table are consistent with the viscosity temperature trend displayed in Figs. 4 to 6. Specifically, it shows that the shear independent viscosity (K), otherwise known as the flow consistency index, decreased between 25 °C and 50 °C and increased afterwards — from 70 °C to 120 °C — for the WBM.

In addition, the calculated E_a was found negative for the WBM, since the flow consistency index increased at higher temperatures. Accordingly, as shown in Fig. 7, the apparent viscosities of the fluids can be adequately predicted based on the thermal effect on the viscosity, by using Eqn. 5. Therefore, based on Fig. 1, the rheological data obtained at 120 °C were assumed to represent the newly formed drilling fluids: OBM_TCF and WBM_TCF.

Gravitational Settling Characteristics of Barite Particles Using Stokes Law

The V_t is an important characteristic of particles suspended in a colloidal system. The V_t depends on the liquid properties — such as density and viscosity — and on particle properties, including diameter, density, and shape. Due to collisions between particles and also between particles and the wall, the V_{STH} becomes effective. The V_{STH} of the barite particles in the drilling fluids are compared in Fig. 8. As shown in this figure, for both fluids, the V_{STH} increases with increasing shear rates. This is because the fluids are non-Newtonian and shear thinning with the apparent viscosity decreasing with the shear rates.

Consequently, consistent with the thermal effect of the rheological characteristics, the V_{STH} decreased with increasing temperatures for the WBM due to the thermal effect, which makes the viscosity of WBM tends to increase with increasing temperatures, notably, at 70 °C to 120 °C. The decrease in settling velocity is an indication of the possibility of lower barite sagging potential in the WBM, as the temperature increases above 70 °C. At higher temperatures 70 °C to 120 °C, the WBM has reduced settling velocity. It can be inferred from these observations that the newly formulated drilling fluid, WBM_TCF, would have exhibited a lower sagging potential of barite particle since the viscosity would increase as the temperature increases from 70 °C to 120 °C. The overall observation presently discussed is consistent with the particle Reynolds number, N_{Rep}, previously presented in Table 2.

CFD Analyses of Barite Settling Characteristics

Mass Fraction and Particle Flux Distributions: Complex flow profiles can arise from a balance of gravitational flux on the particles, which can lead to segregation, with shear-induced migration, causing remixing when particles are subjected to the action of a moving fluid[22]. In other words, the particles experience both buoyancy and the shear-induced effects. Under the typical conditions, it has been experimentally and theoretically shown that the downward gravitational particle flux is balanced by a corresponding upward flux due to shear-induced particle diffusion[20, 22].

Figures 9a and 9b are 2D diagrams showing the description of the general distribution of a mass fraction of the dispersed barite particle at different rotational speeds, 3 rpm to 600 rpm. From Fig. 9a, initially, at time $(t) = 0$, the particles can be seen at the top of the device. Essentially, it shows that the concentration of particles dispersed increases as the pipe rotation rate (rpm) speed increases, and becomes more intense with time; Fig. 9b,

Fig. 5 *A rheogram of the OBM at different temperatures.*

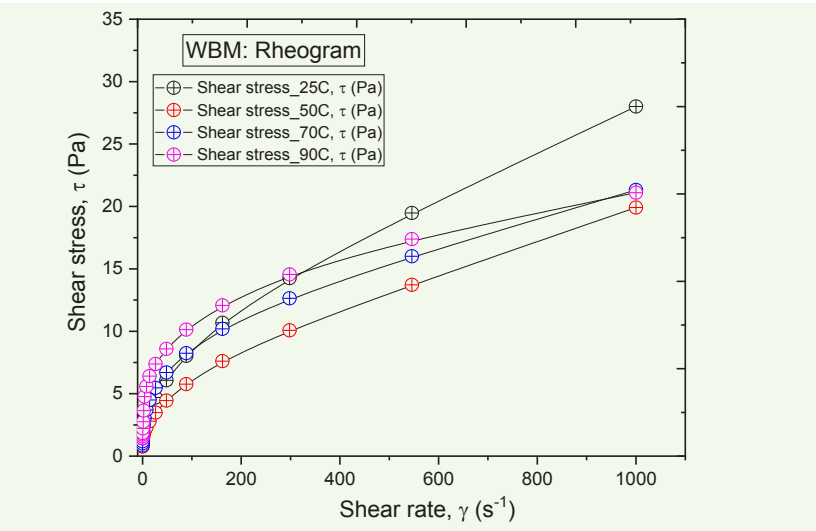

Fig. 6 *The apparent viscosity of OBM and WBM at a constant shear rate (γ = 200 s⁻¹) and different temperatures.*

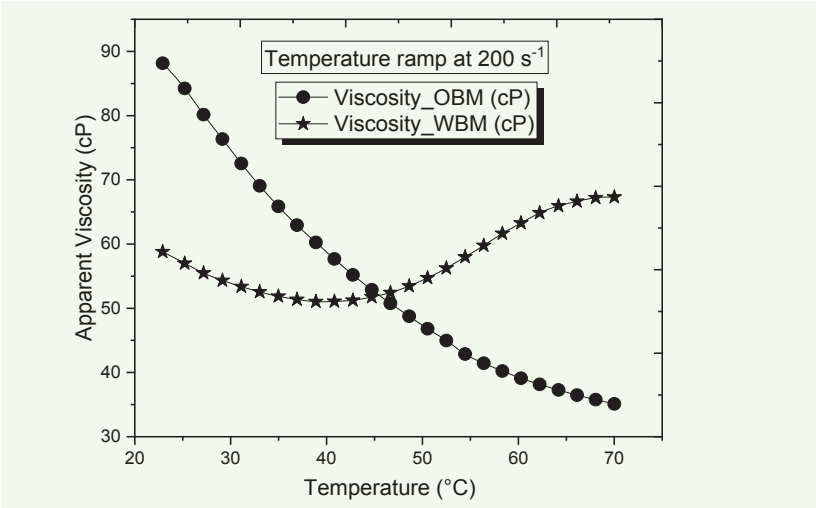

Table 2 *The estimated rheological parameters of the drilling fluids.*
**Note: The properties of the WBM_TCF were obtained at 120 °C.*

	WBM				
T (°C)	N_{Rep}	*K*	*n*	*Ko*	*Ea*
25	1.7E-12	1,591	0.13	12,726	-5,302
50	4.6E-12	1,621	0.27	—	—
70	3.8E-12	1,911	0.29	—	—
90	9E-13	2,347	0.18	—	—
*120	6E-13	3,408	0.20	—	—

Fig. 7 *The predicted apparent viscosity of WBM vs. shear rates at different temperatures based on the thermal effect using Eqn. 5.*

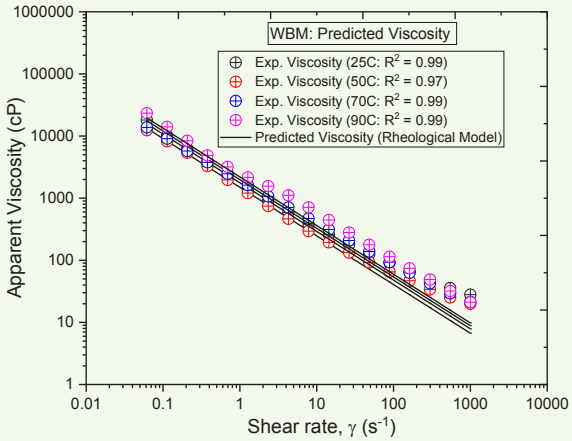

Fig. 8 *The V_{STH} of the barite particles at different temperatures. W_{f1} and W_{f2} represent the behaviors of the WBM and WBM_TCF, respectively.*

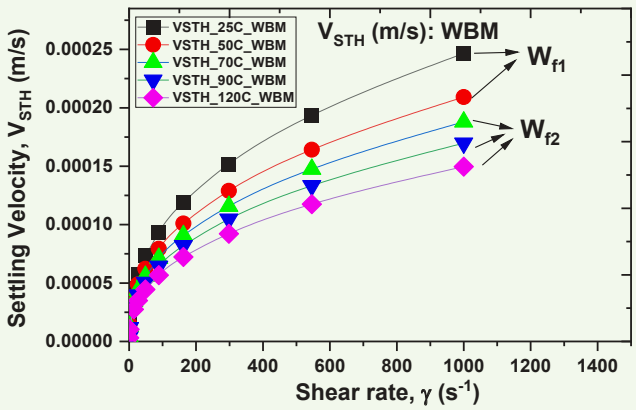

Fig. 9a *A 2D diagram showing the distribution of a mass fraction of barite particles at different rotation rates at an initial time (0 hour).*

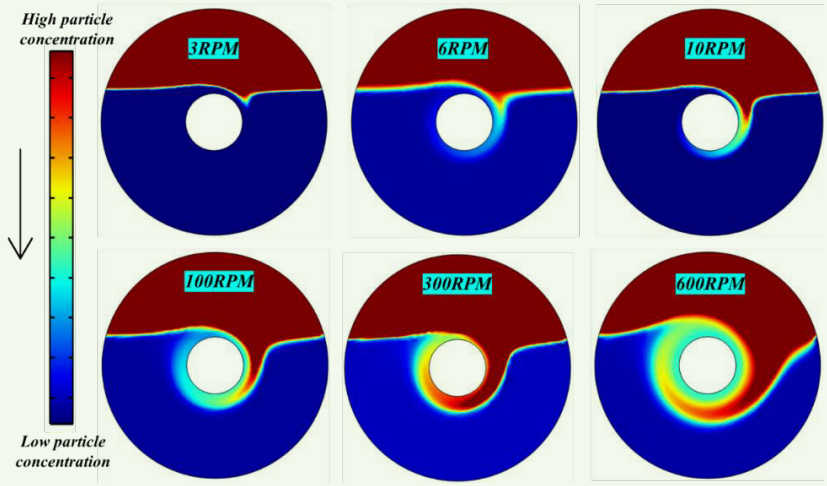

Fig. 9b *A 2D diagram showing the distribution of a mass fraction of barite particles at different rotation rates after 1 hour.*

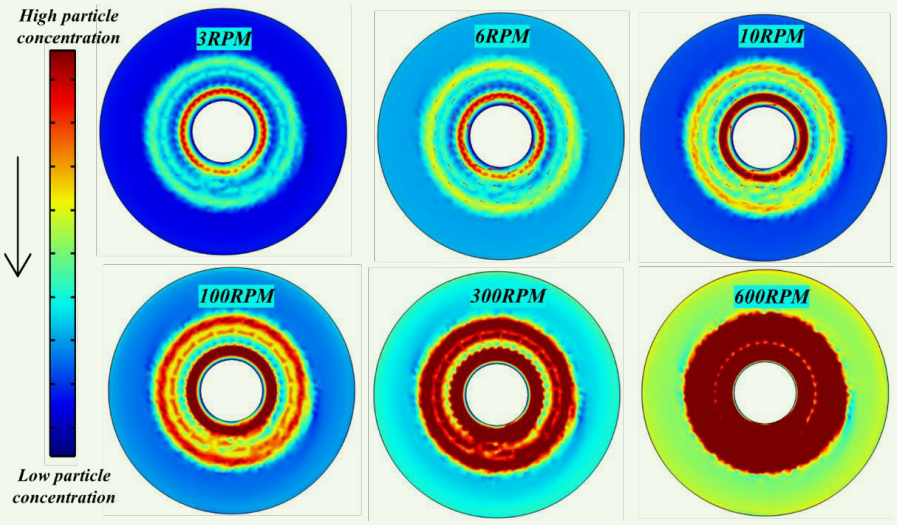

Fig. 10 *The distribution of a mass fraction of barite particles segregated at different rotation rates for WBM.*

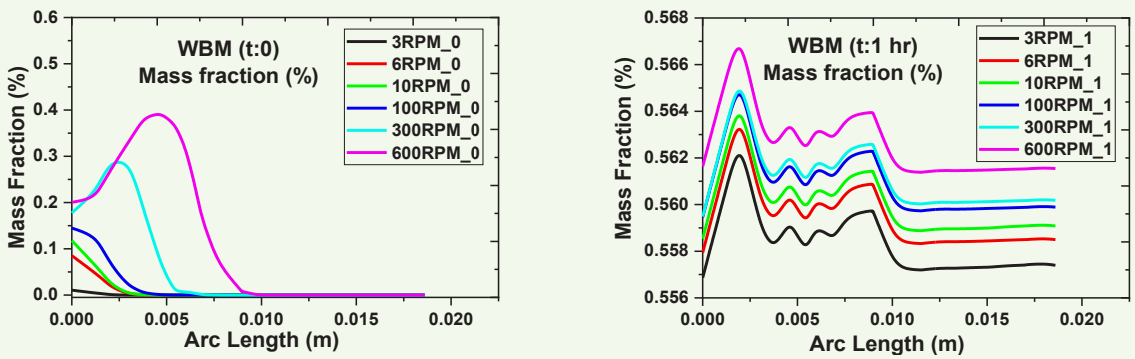

Fig. 11 *The distribution of mass fraction of barite particles segregated at different rotation rates for WBM_TCF.*

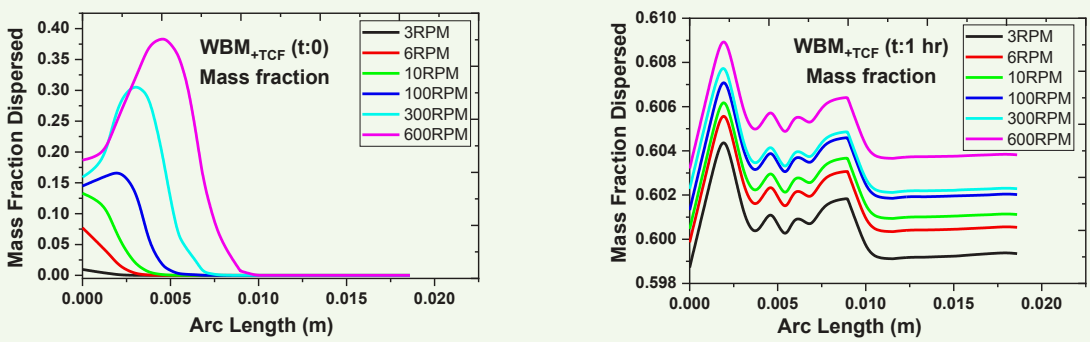

Fig. 12 *The barite particle flux distribution at different rotation rates for WBM.*

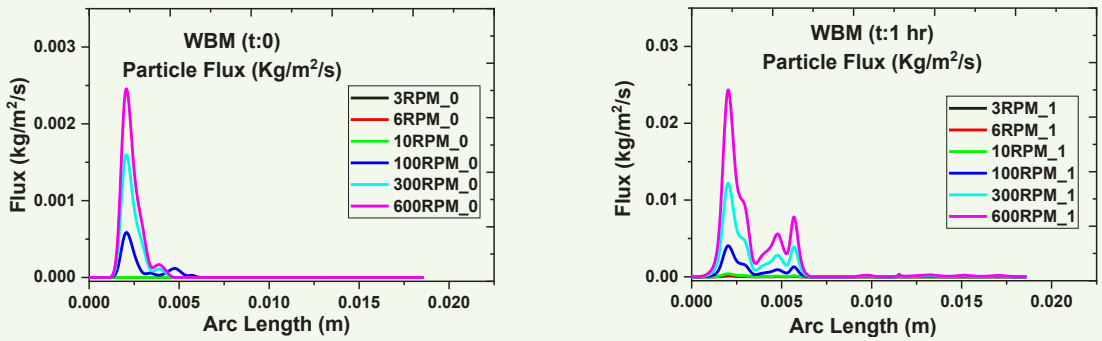

Fig. 13 *The barite particle flux distribution at different rotation rates for WBM_TCF.*

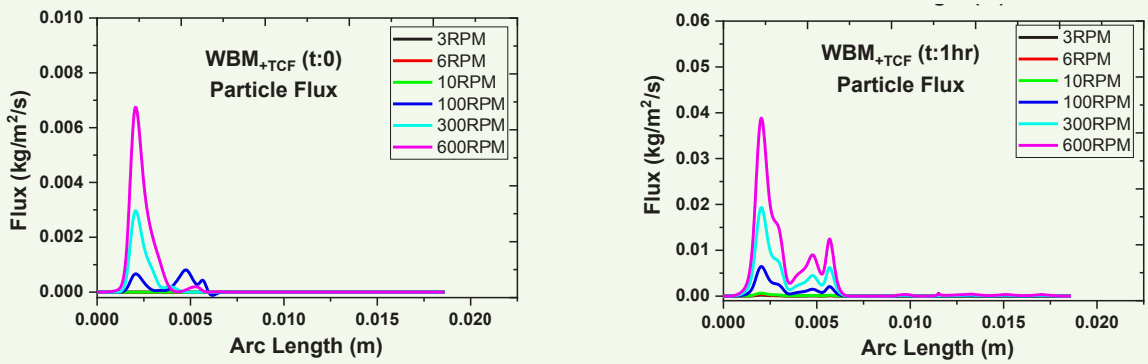

Fig. 14 *The viscosity distribution at different rotation rates for WBM.*

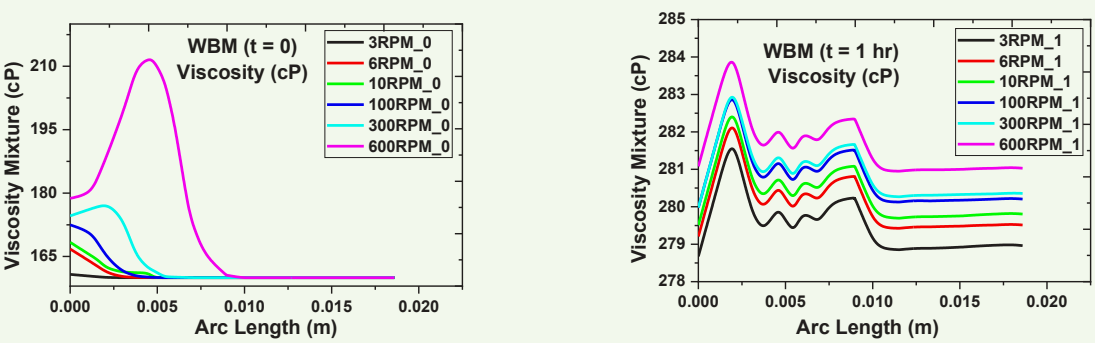

after 1 hour of rotation. In addition, it can be observed that the heavier barite particles tend to move toward the center of rotation in all cases.

Due to shear-induced migration[26] and buoyancy[22], it is expected for flow in a Couette geometry that the particles migrate to the region away from the center of rotation, which experiences a higher rate of rotation to regions away from the center where mixing of bulk fluid is less intense. As seen in the present case, the denser barite particles tend to move toward the center as a lower concentration is observed at the region away from the center of rotation. This could be because the weight force and/or the gravitational effect could probably supersede the shearing force, which causes the particle to migrate, since barite particles are denser that the carrier fluid.

The detailed numerical information of the mass fraction

Fig. 15 *The viscosity distribution at different rotation rates for WBM_TCF.*

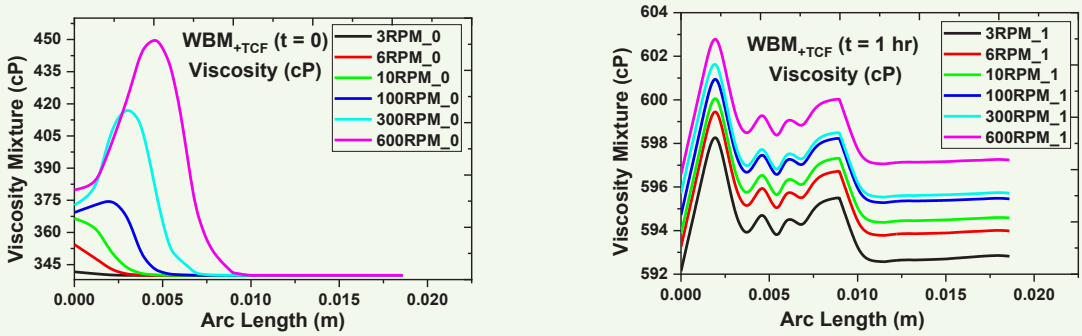

Fig. 16 *A comparison of the pressure drop distribution at different rotation rates for WBM and WBM_TCF.*

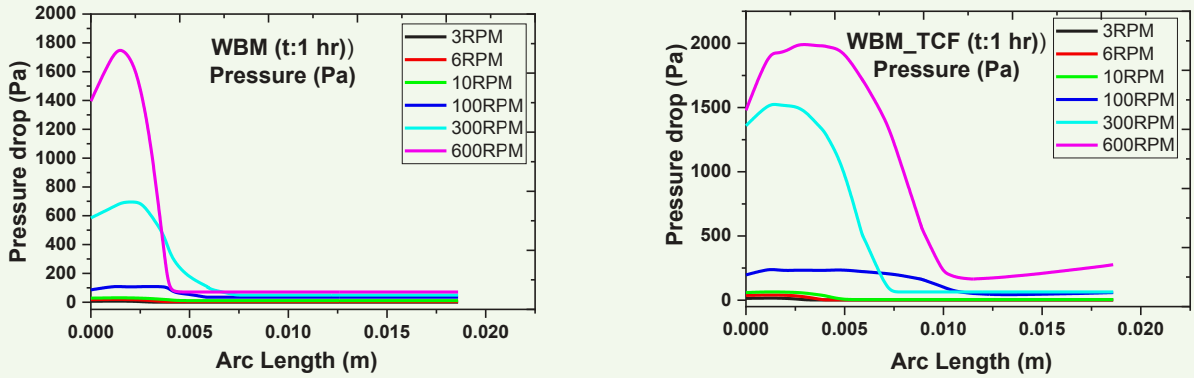

distribution is presented in 1D plots, Figs. 10 and 11. As explained earlier, the figures generally show that the dispersed mass fraction increased with the pipe rotation rate (rpm). It can also be observed that the magnitude of mass fraction initially increased from the edge of the geometry, reached the maximum value at the center, and decreased afterwards. Specifically, the mass distribution patterns for the WBM and those of the newly formulated WBM_TCF are presented in Figs. 10 and 11, respectively.

From Fig. 10, at $t = 0$, it can be observed that the WBM (top) exhibits a similar mass fraction distribution (maximum value of 0.39 at 600 rpm). Subsequently, when generally compared, the WBM_TCF has the highest value of mass fraction of ≈0.601, Fig. 11 bottom. This observation can be reasonably linked with the rheological characteristics of the WBM_TCF and the response of its viscosity to shear rates at higher temperatures, which has been discussed earlier. Similarly, it can be inferred from the presented mass fraction distribution patterns, that the WBM_TCF would have exhibited a lower sagging potential of barite particle since the viscosity would increase as the temperature increases from 70 °C to 120 °C, therefore, more particles would be carried in the liquid phase.

Particle migration has been reported to be induced by three factors, including gradients in shear rate, concentration, and relative viscosity[22], and the argument has been referenced as a basis for developing a diffusive flux model, which has been employed in the viscous resuspension phenomenon[21]. The flux of dispersed barite particles, Fig. 12 for WBM, and Fig. 13 for WBM_TCF, generally shows that the particle flux increases with the pipe rotation rate (rpm) and time. In addition, it shows that there is a possibility of higher flux at the region close to the axis of rotation within the geometry, compared to the region far away from the axis of rotation where the flux is the same and apparently flattens out regardless of the rotation rates. It can be observed that the newly developed mud, WBM_TCF, has a higher particle flux compared with the WBM.

Viscosity Distribution and Pressure Drop: The viscosity fluid has a significant impact on barite segregation. Therefore, it is widely believed[2, 13, 27], that barite settling can be effectively minimized through the modification of rheological properties and/or improving the viscosity. Accordingly, the viscosity profiles displayed in Figs. 14 and 15, for WMB and WBM_TCF, respectively, corroborates the barite segregation patterns that have been previously discussed.

In the Couette geometry, the shear rate varies radially

across the distance, and this influences the particle distribution as well as other bulk properties of the fluid such as viscosity and pressure drop. As generally seen in these results, the viscosity variation followed a similar pattern. It can be clearly observed that the viscosity of the mixture increases as the pipe rotation increases. This is so because the fraction of the dispersed barite particles increased with the pipe rotation. It can be observed that the WBM has a maximum viscosity of 210 cP, which increased to ≈284 cP.

In comparison, the WBM_TCF exhibits the maximum viscosity of ≈450 at t = 0, which increased to ≈600 cP after 1 hour of pipe rotation. More so, the results displayed in Fig. 16 show that the WBM_TCF would experience higher pressure drops compared with the WBM.

Conclusions

In this investigation, the barite segregation potential of WBM and the one containing a TCF additive, WBM_TCF, has been investigated. Experimental studies of the rheological characteristics as well as numerical simulation using CFD was conducted.

The results from the rheological studies as well as the CFD can be summarized as:

1. The drilling fluid conforms to the shear thinning pseudoplastic behavior with the conditions operated in this study.
2. The apparent viscosity of the WBM decreased with an increasing temperature between 25 °C and 50 °C, while the apparent viscosity increased afterward; 70 °C to 120 °C.
3. Evaluation of gravitational settling characteristics revealed that the WBM_TCF has a lower barite settling velocity compared with the conventional WBM, due to the reaction of the TCF, which raises the temperature and increases the viscosity.
4. In addition, the CFD studies have considered both the hydrodynamic forces and shear-induced migration of the particles. Analyses of various simulation results, including particle flux, particle mass fraction, mixture viscosity, and the pressure drop, consistently revealed that the WBM_TCF might have a lower barite segregation potential compared with the WBM.

References

1. Welahettige, P., Lie, B. and Vaagsaether, K.: "Computational Fluid Dynamics Study of Shear Thinning Fluid (Drilling Fluid) Viscosity Models in an Open Venturi Channel," *International Journal of Petroleum Science and Technology*, Vol. 13, Issue 1, March 2019, pp. 9-20.
2. Ofei, T.N., Lund, B., Saasen, A., Sangesland, S., et al.: "Barite Sag Measurements," SPE paper 199567, presented at the IADC/SPE International Drilling Conference and Exhibition, Galveston, Texas, March 3-5, 2020.
3. Skalle, P., Backe, K.R., Lyomov, S.K. and Sveen, J.: "Barite Segregation in Inclined Boreholes," *Journal of Canadian Petroleum Technology*, Vol. 38, Issue 13, December 1999.
4. Mohamed, A., Basfar, S., Elkatatny, S. and Al-Majed, A.: "Prevention of Barite Sag in Oil-Based Drilling Fluids Using a Mixture of Barite and Ilmenite as Weighting Material," *Sustainability*, Vol. 11, Issue 20, October 2019.
5. Mohamed, A.K., Elkatatny, S.A., Mahmoud, M.A., Shawabkeh, R.A., et al.: "The Evaluation of Micronized Barite as a Weighting Material for Completing HPHT Wells," SPE paper 183768, presented at the SPE Middle East Oil and Gas Show and Conference, Manama, Kingdom of Bahrain, March 6-9, 2017.
6. Basfar, S., Elkatatny, S., Mahmoud, M., Kamal, M.S., et al.: "Prevention of Barite Sagging while Drilling High-Pressure High Temperature (HPHT) Wells," SPE paper 192198, presented at the SPE Kingdom of Saudi Arabia Annual Technical Symposium and Exhibition, Dammam, Kingdom of Saudi Arabia, April 23-26, 2018.
7. Bern, P.A., van Oort, E., Neustadt, B., Ebeltoft, H., et al.: "Barite Sag: Measurement, Modeling, and Management," *SPE Drilling & Completion*, Vol. 15, Issue 1, March 2000, pp. 25-30.
8. Pereira, F.A.R., Barrozo, M.A.S. and Ataíde, C.H.: "CFD Predictions of Drilling Fluid Velocity and Pressure Profiles in Laminar Helical Flow," *Brazilian Journal of Chemical Engineering*, Vol. 24, Issue 4, December 2007, pp. 587-595.
9. Hanson, P.M., Trigg Jr., T.K., Rachal, G. and Zamora, M.: "Investigation of Barite 'Sag' in Weighted Drilling Fluids in Highly Deviated Wells," SPE paper 20423, presented at the SPE Annual Technical Conference and Exhibition, New Orleans, Louisiana, September 23-26, 1990.
10. Omland, T.H., Saasen, A. and Amundsen, P.A.: "Detection Techniques Determining Weighting Material Sag in Drilling Fluid and Relationship to Rheology," *Annual Transactions of the Nordic Rheology Society*, Vol. 15, 2007, pp. 1-9.
11. Parvizinia, A., Ahmed, R.M. and Osisanya, S.O.: "Experimental Study on the Phenomenon of Barite Sag," IPTC paper 14944, presented at the International Petroleum Technology Conference, Bangkok, Thailand, November 15-17, 2011.
12. Nguyen, T., Miska, S., Yu, M., Takach, N., et al.: "Experimental Study of Dynamic Barite Sag in Oil-Based Drilling Fluids Using a Modified Rotational Viscometer and a Flow Loop," *Journal of Petroleum Science and Engineering*, Vol. 78, Issue 1, July 2011, pp. 160-165.
13. Dye, W., Hemphill, T., Gusler, W. and Mullen, G.: "Correlation of Ultralow Shear Rate Viscosity and Dynamic Barite Sag," *SPE Drilling & Completion*, Vol. 16, Issue 1, March 2001, pp. 27-34.
14. Marshall, D.S.: "Laboratory Investigation of Barite Sag in Drilling Fluids," *Annual Transactions of the Nordic Rheology Society*, Vol. 15, 2007.
15. Zakerian, A., Sarafraz, S., Tabzar, A., Hemmati, N., et al.: "Numerical Modeling and Simulation of Drilling Cutting Transport in Horizontal Wells," *Journal of Petroleum Exploration and Production Technology*, Vol. 8, January 2018, pp. 455-474.
16. Tariq, Z., Kamal, M.S., Mahmoud, M., Alade, O., et al.: "Self-Destructive Barite Filter Cake in Water-Based and Oil-Based Drilling Fluids," *Journal of Petroleum Science and Engineering*, Vol. 197, February 2021.
17. de Waele, A.: "Viscometry and Plastometry," *Journal of the Oil and Color Chemists' Association*, Vol. 6, Issue 38, 1923, pp. 33-69.
18. Ostwald, W.: "Uber die Geschwindigkeitsfunktion der Viskosit¨at disperser Systeme. I," *Colloid and Polymer Science*, Vol. 36, 1925, pp. 99-117.

19. McCabe, W.L., Smith, J.C. and Harriott, P.: *Unit Operations of Chemical Engineering*, McGraw-Hill, New York, 1993, 1,088 p.

20. Acrivos, A., Batchelor, G.K., Hinch, E.J., Koch, D.L., et al.: "Longitudinal Shear-Induced Diffusion of Spheres in a Dilute Suspension," *Journal of Fluid Mechanics*, Vol. 240, July 1992, pp. 651-657.

21. Phillips, R.J., Armstrong, R.C., Brown, R.A., Graham, A.L., et al.: "A Constitutive Equation for Concentrated Suspensions that Accounts for Shear-Induced Particle Migration," *Physics of Fluids A: Fluid Dynamics*, Vol. 4, Issue 1, 1992.

22. Rao, R., Mondy, L., Sun, A. and Altobelli, S.: "A Numerical and Experimental Study of Batch Sedimentation and Viscous Resuspension," *International Journal for Numerical Methods in Fluids*, Vol. 39, Issue 6, June 2002, pp. 465-483.

23. COMSOL: "Multiphase Flow Interfaces," Chapter 6 in *Multiphysics 5.6 CFD Module User's Guide*, 2020, 862 p.

24. Bird, R.B., Stewart, W.E. and Lightfoot, E.N.: *Transport Phenomena*, John Wiley & Sons, New York, 2007, 928 p.

25. Alade, O.S.: "Rheological Modeling of Complex Flow Behavior of Bitumen-Solvent Mixtures and Implication for Flow in a Porous Medium," *Journal of Energy Resources Technology*, Vol. 144, Issue 7, July 2022, pp. 073004-073015.

26. Murisic, N., Pausader, B., Peschka, D. and Bertozzi, A.L.: "Dynamics of Particle Settling and Resuspension in Viscous Liquid Films," *Journal of Fluid Mechanics*, Vol. 717, February 2013, pp. 203-231.

27. Ribeiro Jr., J.M., Eler, F.M., Martins, A.L., Scheid, C.M., et al.: "A Simplified Model Applied to the Barite Sag and Fluid Flow in Drilling Muds: Simulation and Experimental Results," *Oil & Gas Science and Technology — Rev. IFP Energies Nouvelles*, Vol. 72, Issue 4, July-August 2017.

About the Authors

Dr. Olalekan Alade

Ph.D. in Earth Resources Engineering, Kyushu University

Dr. Olalekan Alade joined the Department of Petroleum Engineering, College of Petroleum and Geosciences, King Fahd University of Petroleum and Minerals, (KFUPM), Dhahran, Saudi Arabia, in May 2018, as a Postdoctoral Fellow. He currently works as a Research Engineer at the Center for Integrative Petroleum Research (CIPR) of the College.

Olalekan's research interest spans the application of principles of chemical and petroleum engineering, including fluid dynamics, transport phenomenon, thermodynamics, and reaction engineering in solving various problems in the aspects of petroleum recovery, flow, and transportation.

In 2017, he received his Ph.D. degree in Earth Resources Engineering from Kyushu University, Fukuoka, Japan, with a specialty in heavy oil resources production and safety engineering.

Dr. Mohamed Mahmoud

Ph.D. in Petroleum Engineering, Texas A&M University

Dr. Mohamed Mahmoud is a Professor working in the Department of Petroleum Engineering at King Fahd University of Petroleum and Minerals (KFUPM), Dhahran, Saudi Arabia. His areas of research include carbonate and sandstone stimulation, formation damage, and rock petrophysics and geomechanics.

Mohamed has authored or coauthored several journal and conference papers, in addition to more than 80 U.S. patents.

He received both his B.S. degree and M.S. degree in Petroleum Engineering from Suez Canal University, Ismailia, Egypt. Mohamed received his Ph.D. degree in Petroleum Engineering from Texas A&M University, College Station, TX, in 2011.

Ayman R. Al-Nakhli

M.S. in Entrepreneurship for New Business Development, Open University Malaysia

Ayman R. Al-Nakhli is a Petroleum Scientist in Saudi Aramco's Exploration and Petroleum Engineering Center – Advanced Research Center (EXPEC ARC), where he leads the research program on thermochemicals and develops technologies related to conventional and unconventional reservoirs such as pulse fracturing, stimulation, diverting agents, and heavy oil.

Ayman has developed and field deployed several novel technologies, with four of them being commercialized with international service companies. He received the World Oil Award for Best Production Chemical in 2015.

Ayman has filed more than 20 patents, published 35 journal papers, and 40 conference papers.

He received his B.S. degree in Industrial Chemistry from King Fahd University of Petroleum and Minerals (KFUPM), Dhahran, Saudi Arabia, and an M.S. degree in Entrepreneurship for New Business Development from Open University Malaysia, Bahrain.